Title
Analytical and numerical solutions of hydrometeor momentum equations

Journal
Quarterly Journal of the Royal Meteorological Society

ISSN
0035-9009

Authors
Wu, Samuel
Igel, Matthew R
Igel, Adele L
et al.

Publication Date
2026-08-26

DOI
10.1002/qj.70283

ORIGINAL ARTICLE

Journal Section

Analytic and Numeric Solutions of Hydrometeor Momentum Equations

Samuel Wu[1] | Matthew R. Igel[2] | Adele L. Igel[3] | David H. Marsico[4,5]

[1]Department of Physics and Astronomy, University of California Davis

[2]Department of Land, Air and Water Resources, University of California Davis

[3]Department of Land, Air and Water Resources, University of California Davis

[4]Cooperative Institute for Research in Environmental Science, University of Colorado-Boulder

[5]NOAA Physical Sciences Laboratory, Boulder CO

Correspondence
Matthew R. Igel, Department of Land, Air and Water Resources, University of California Davis, Davis, CA, 95616, USA
Email: migel@ucdavis.edu

Funding information
National Science Foundation Division of Geosciences 2025103

Momentum equations of hydrometeors and air variously forced by gravity and frictional dissipation are considered. Limiting cases are shown to reveal important behavior. The case of hydrometeors accelerating to the velocity of a constant horizontal wind reveals extremely long equilibration times due to friction alone. Velocity traces for the case of accelerating hydrometeors falling through air and the case of accelerating hydrometeors and air under the influence of gravity are found. They reveal that acceleration occurs for about twice as long as naive scaling would suggest. When the laden system can accelerate both horizontally and vertically, the solution to momentum equations is complicated by the unique vector nature of the problem. Numerical solutions illustrate how drops act as a damper on the motion of air. A particular focus throughout is on the modification of terminal hydrometeor fall speeds due to multiple effects. Among these are enervation due to accounting for hydrometeor momentum, invigoration from viscous effects for the very smallest drops, and enervation from relative horizontal motion of particles during settling.

KEYWORDS
Momentum Equations, Hydrometeors, Hydrometeor Loading

* S.W. found solutions. M.I., A.I. and D.M. performed additional analysis. S.W. and M.I. wrote the manuscript. A.I. secured funding.

Introduction and Motivation

In the simplest sense, understanding weather is the process of understanding where moist air rises, saturates, and precipitates. Yet, none of these steps is simple. The first involves understanding complicated dynamics and the second, complicated thermodynamics. The complexity of these two steps has spurred whole branches of atmospheric science. The third step is often (but not always) treated simply by assuming drops fall at a constant speed or sometimes even trivially by assuming drops fall out of the atmosphere instantaneously. The constant fall speed approximation is typically justified by recognizing that gravity accelerates drops very quickly to a terminal speed at which frictional dissipation with the air perfectly balances the gravitational attraction to the surface. Because of Newton's Third Law, the air through which the drops pass is accelerated downward at the weight of the hydrometeor.

However, treating hydrometeor settling this simply precludes understanding of possibly important behavior of drops and their coupling with air motions. For example, Makarieva *et al.* (2017) recently pointed out an important inconsistency in different formulations of momentum equations of moist air in Ooyama (2001) and Bannon (2002) regarding the "reactive motion" of a newly laden system – essentially a fundamental difference in how the air behaves in the presence of new, falling drops. Stout *et al.* (1995) considered the settling dynamics of heavy drops reacting to prescribed turbulent atmospheric flows and showed that "subterminal" settling, a drop falling at a speed below its size-determined terminal speed, is expected due to the odd nature of friction (discussed below as well). Ingel' (2012) showed a similar result for drops in shear flows, and Shapiro (2005) showed that horizontal exchange of momentum between drops and the air can lead to vertical flux of horizontal momentum.

From cloud dynamics and cloud physics perspectives, there are a few reasons to consider the consequences of hydrometeor accelerations. As the above-cited studies suggest, the detailed physics that govern hydrometeor motions may be particularly important in turbulent air where hydrometeors motions can be non-terminal and where there are feedbacks to air motions. The exact motion of hydrometeors will also impact microphysical processes such as collision-coalescence rates. From a modeling standpoint, we believe the question of hydrometeor motion needs to be revisited as contemporary simulations are run at ~100 m scales. As we will show in what follows, hydrometeor accelerations should probably be considered in simulations with timesteps of ~1 s or less. Some DNS models account for acceleration of cloud droplets already through the use of a relaxation method [e.g. (Chen *et al.*, 2018)] but more widespread inclusion of hydrometeor acceleration may be needed. Finally, practical concerns aside, we are motivated simply from curiosity to develop a more complete understanding of this coupled system.

Our basic goal below is to construct equations of motion for individual hydrometeors in air and to thereby understand the evolution of air laden with hydrometeors in cloudy systems. Separating our analysis from those mentioned above, one of the novelties of our development below is that we address this goal by starting with the simplest possible case and building complexity systematically. The simplest system is solved analytically and interpreted. The most complicated system is solved numerically. Systems in between allow some analytic and some numerical treatment. Our foci are on the importance of explicit momentum of hydrometeors and the impact of the vector nature of frictional dissipation. The first focus helps us better understand hydrometeor loading – the first order way in which the air feels the effects of friction. The second focus helps us better understand that hydrometeor settling must be considered in the context of the full wind. This work aims to provide a deeper discussion than is currently available in the atmospheric science literature.

Dynamics

| Important Assumptions

First, hydrometeors are assumed to be round and rigid spheres. They do not break up, nor do they dissipate energy internally through internal waves. Second, we neglect the buoyancy of hydrometeors. In principle, solid or liquid balls should displace a mass of air equivalent to their volume multiplied by the density of air, but for dense objects in a low-density fluid like water or ice in air at atmospheric pressures, this effect is small (Loftus and Wordsworth, 2021). Third, individual hydrometeors will not interact dynamically through collisions. Even in the final section, when we consider solutions for distributions of hydrometeor sizes, the individual hydrometeors each act individually on the air, and their effects are simply summed. Fourth, we always assume that the air is hydrostatically balanced. That is to say, the vertical pressure gradient force always perfectly balances the gravitational attraction of the air even though new hydrometeor formation subtly affects the background pressure field (Spengler *et al.*, 2011). Crucially, we also assume that the momentum of hydrometeors is non-negligible. The opposite assumption is often made in practice, especially in models (Pielke Sr., 1984). Finally, for numerical calculations, the density of air, ρ_a, used in calculations is 1.22 kg m^{-3} unless otherwise noted, and the kinematic viscosity of air, μ, is $1.57(10^{-5})m^2s^{-1}$.

An additional assumption is made to avoid the difficulty in dealing with momentum equations for moist air with phase changes (Makarieva *et al.*, 2017; Ooyama, 2001; Bannon, 2002). We will always assume that hydrometeors start from rest upon their formation so we can treat all cases similarly. This allows us to focus our attention on the motion of long-lived hydrometeors but at the cost of an incomplete thermodynamic coupling.

Finally, in order not to complicate our goals, the authors ignore stochastic processes observed and known to affect the instantaneous motion and net settling of hydrometeors. These include processes like “loitering”, “sweeping”, and “fast-tracking” which may depend sensitively on the geometry of real hydrometeors or on the geometry of turbulent eddies (Maxey, 1987; Montero-Martínez *et al.*, 2009; Good *et al.*, 2014; Garrett *et al.*, 2025). To treat all these processes well requires detailed methods and regime dependent examination. Both are beyond the goal of this paper, which is more macroscopic in nature.

| Parameterizing Friction

The simplest way to approximate the friction of a sphere moving in a fluid is to employ an empirical drag coefficient, *C*, and to use the equation

$$\|\mathbf{F_f}\| = m\frac{1}{2}\rho_a v^2 C\pi r^2 \tag{1}$$

where *F* is a force, the subscript *f* implies friction, *m* is the mass of the sphere, ρ is a density, the subscript *a* is used for the air, *v* is the velocity of the sphere, and *r* is the radius of the sphere (Shapiro, 2005; Khain and Pinsky, 1995). The simplicity of this equation pushes the burden of the complexity of friction onto *C*. The drag coefficient typically depends on the value of the Reynolds number $Re = \frac{2\rho_a r v}{\mu}$ which itself depends on the radius and velocity of the falling object and μ. The dependence of the drag coefficient on the Reynolds number changes with radius, leading to different regimes [usefully discussed in Amanbaev (2024) and Pruppacher and Klett (1997)]. The first regime, which applies when *Re* << 1, is the Stokes' regime, where flow around the particle is generally streamlined and laminar, results in a F_f that is linearly proportional to the relative velocity, and thus inversely proportional to the Reynolds number. A second regime applies when *Re* >> 1 and the flow around the droplets in this case is far more nonlinear and includes turbulence in the wake of the droplet. Amanbaev (2024) refers to this regime as the Newtonian regime and assumes a constant drag coefficient in this regime. There is also an intermediate range of sizes where neither regime applies well which may be referred to as the “intermediate regime”.

We choose to use a relatively simple parameterization of C which accounts for these different regimes, yet which remains mathematically tractable in all cases.

$$C = \overbrace{\frac{24}{Re}}^{\text{Stokes}} + \overbrace{\frac{4.4}{\sqrt{Re}}}^{\text{Intermediate}} + \overbrace{0.44}^{\text{Newtonian}} \tag{2}$$

This parameterization from Amanbaev (2024) is conceptually convenient because it is clear which terms dominate in which physical regime [labeled in (2)].

| Relevant Physics

Throughout the discussion of physically limited cases below, Figure 1 will serve as a simple illustration of the appropriate physical system for each case. Having neglected buoyancy (see above), the only relevant forces are friction and gravity. The force of gravity is $\mathbf{F_g} = g\mathbf{k}$ since we are working in a per unit mass sense for force by convention.

Beginning with (1) and noting the relationships among drop density, cross-sectional area, and volume, the frictional force (per unit mass from now on to follow convention) commonly used is

$$\mathbf{F_f} = -\frac{3}{8}\frac{\rho_a}{\rho_w}\frac{1}{r}C\|\mathbf{v_c} - \mathbf{v_a}\|(\mathbf{v_c} - \mathbf{v_a}) \tag{3}$$

where $\boldsymbol{v}$ is the vector velocity with two components $\mathbf{v} = u\mathbf{i} + w\mathbf{k}$ where $\mathbf{i}$ is defined by the plane of 2-dimensional hydrometeor motion with $\mathbf{k}$, ρ_w is the density of water (liquid or ice; liquid is always assumed below), and the subscript c denotes condensate. It's worth considering the vector nature of (3). The absolute value term implies that any component of the frictional force is proportional to the total vector difference of the velocity. This makes sense if we imagine that friction between a hydrometeor and the air is due to the generation and dissipation of vortices in the wake of the particle. Stout *et al.* (1995) and Shapiro (2005) point out that this can result in unintuitive effects like horizontal winds slowing the vertical fall speed of a droplet – effects that will be missed if the components are treated separately. The term in parentheses implies that the magnitude of the frictional force in a particular direction is additionally proportional to the relative velocity of the air and the hydrometeor in that direction.

Further complicating the nature of the friction, the empirical drag coefficient, C, depends explicitly on the relative velocity (given a subscript r and defined simply as $\mathbf{v_r} = \mathbf{v_c} - \mathbf{v_a}$) as

$$C = \frac{12\mu}{\rho_a r\|\mathbf{v_r}\|} + 4.4\sqrt{\frac{\mu}{2\rho_a r\|\mathbf{v_r}\|}} + 0.44 \tag{4}$$

To simplify this problem, Stout *et al.* (1995) suggested always using a specific velocity when calculating C. That velocity should be chosen to reduce the complexity of the problem. Throughout most of what follows, we employ the “terminal drag coefficient”, C_T, which is C calculated using the terminal fall speed (which we will show is situationally

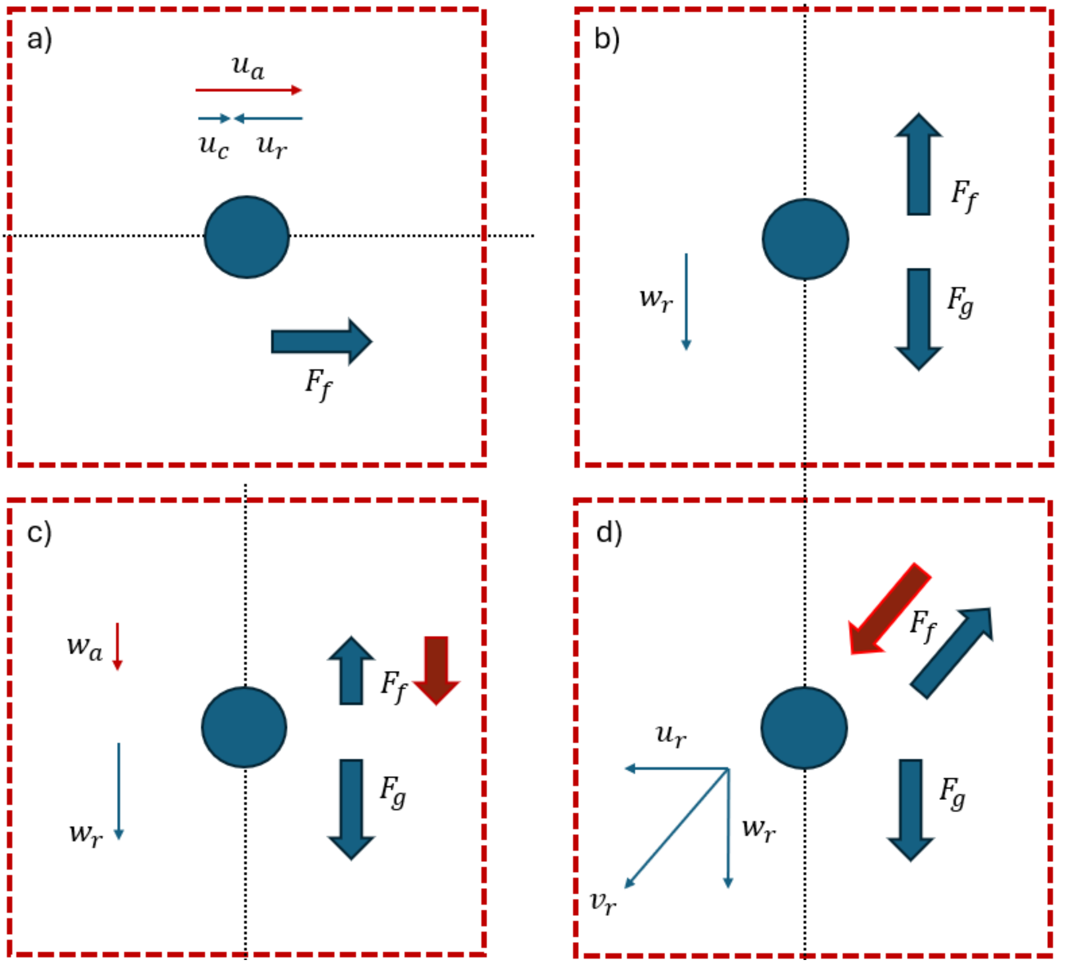

FIGURE 1 *Schematic representations of various physically limiting cases considered. Bold vectors indicate forces and thin arrows show velocities. Blue coloring indicates properties pertaining to hydrometeors and red coloring is used for the air.*

dependent). This is done so that analytic solutions to momentum equations become tractable. Details on how C_T is calculated and the magnitude of errors introduced in so doing are included in Appendix A.

Given our assumptions (including hydrostatic balance) and the physics laid out, the only force acting on the air that we need to consider is friction with hydrometeors. By Newton's Third Law, it is calculated by changing the order of the velocity differencing in (3). The only forces acting on hydrometeors are friction and gravity. In what follows, we make use of three limiting cases before discussing the fully coupled, 2-dimensional case. Each limiting case helps to elucidate some behavior of the full problem more clearly.

| Physical Cases

| Uncoupled Horizontal Case

The simplest case we will discuss is the least physically relevant. It is the case of suspended hydrometeors responding to a horizontal wind (no net forces in the vertical). In essentially all numerical models and conceptual models of which the authors are aware, hydrometeors are assumed to advect horizontally with the air. That is, they act as passive tracers of the horizontal wind. Figure 1a illustrates the relevant physics of this case. The wind blows at a constant value, u_a. If there is a relative horizontal velocity between the hydrometeors and air (i.e. $u_r \neq 0$), then there is a frictional force which accelerates the hydrometeor in the direction of u_a (where the local wind may define the coordinate system). In this case, the equation of motion to solve is

$$\frac{du_c}{dt} = -\frac{3}{8}\frac{\rho_a}{\rho_w}\frac{1}{r}Cu_r\|u_r\| \tag{5}$$

where we have not assumed that $C = C_T$ here since the concept of a terminal velocity is irrelevant when only frictional acceleration enters the problem. The solution to (5) assuming $u_c(0)$=0 m s^{-1} and constant C for clarity is

$$u_c(t) = u_a(1 - [\frac{3\rho_a Ct}{8\rho_w r}u_a + 1]^{-1}) \tag{6}$$

For a first pass, (6) can be easily understood by assuming a constant C appropriate for the Newtonian regime. As time increases, u_c approaches u_a. This occurs faster for smaller hydrometeors and for greater u_a. Illustrative velocity traces using (4) and (6) for hydrometeors beginning at rest and accelerating toward u_a=1 m s^{-1} for several radii are shown in Fig. 2a. Because of the decreasing intensity of friction as u_r approaches 0 m s^{-1}, hydrometeors initially accelerate rapidly toward u_a before entering a period of only asymptotically approaching u_a. In fact, Fig. 2a shows that drops accelerate to 90% of u_a in much less time than they accelerate from 90% of u_a to 99% of u_a. Drops of radii over 1 cm, never reach 99% of u_a in the 1000 s shown which is likely longer than the residence time in the atmosphere. While this is clearly unrealistic given that hydrometeors are observed to have significant u_c, it demonstrates that medium and large hydrometeors may not act as horizontal tracers due to horizontal friction with the air alone and that forces in the vertical on the hydrometeors are necessary to explain their horizontal motion. While we have assumed $u_c(0)$=0 m s^{-1} to illustrate the relevant physics of the system, in reality, new particles are formed at the velocity of their enveloping fluid, however this is the trivial case here. We solve and discuss problems throughout this paper in the way that sheds the most light on the problem, but in all cases different initial conditions can be employed as necessary.

| Uncoupled Vertical Case

Next, we consider the case in the vertical direction without horizontal forces (Fig. 1b). It is

$$\frac{dw_c}{dt} = -\frac{3}{8}\frac{\rho_a}{\rho_w}\frac{1}{r}C_T w_r\|w_r\| - g \tag{7}$$

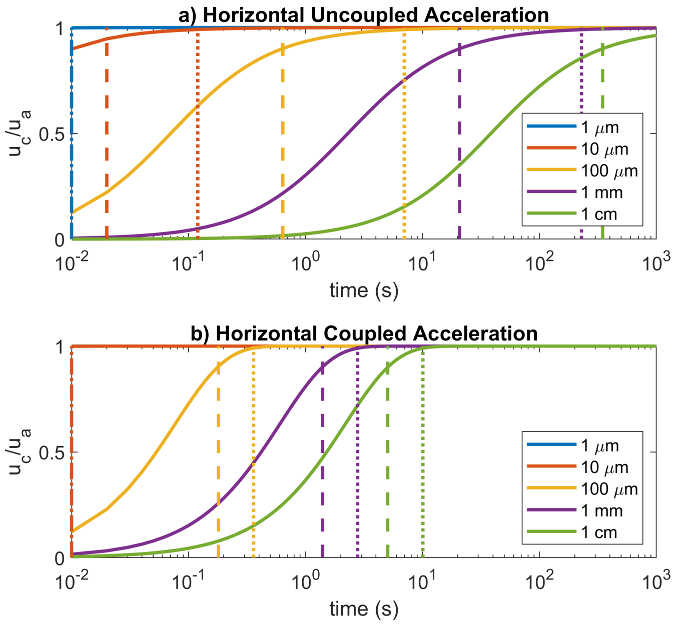

FIGURE 2 *Solid lines show normalized drop velocity as a function of time for* u_a*=1 m s*$^{-1}$*. Dashed lines show when* $\frac{u_c}{u_a} = 0.9$*, and dotted lines shown when* $\frac{u_c}{u_a} = 0.99$*. Panel a) shows solutions to the uncoupled equations, and panel b) shows solutions which assume* $\|\mathbf{v_r}\| = w_T$ *for the coupled equations (note that the blue lines are overlain by the red line).*

where we have employed $C = C_T$ for the first time.

Despite being more complicated than (5) only by the addition of (a constant) gravity, the presence of the absolute value sign requires more consideration here. It results in the sign of the first term of the equation being different, depending on the sign of the quantity w_r. We use the convention that velocity is positive upward, so at the initial time when we assume hydrometeors are still at rest, for updrafts, $w_r(t = 0) < 0$, and for downdrafts, $w_r(t = 0) > 0$. At long times, hydrometeors fall relative to the air around them, so eventually the sign of w_r will be negative. This means that in the downdraft case, after some amount of time the sign of the first term will change, and it will take the same functional form as the updraft case at long times.

First, we can find an expression for the terminal velocity, w_T . The terminal velocity is defined as the value of w_r when $\frac{dw_r}{dt} = 0$ for the case of $v_r < 0$. We will simplify the notation by defining $c_1 = \frac{3\rho_a C_T}{8\rho_w r}$. Substituting c_1, (7) becomes

$$\frac{dw_c}{dt} = -c_1 w_r \|w_r\| - g \tag{8}$$

Noting in this case that $\frac{dw_c}{dt} = \frac{dw_r}{dt}$, the terminal velocity is found to be

$$w_T(r,\rho_a) = \sqrt{\frac{g}{c_1}} = \sqrt{\frac{8\rho_w r g}{3\rho_a C_T}} \tag{9}$$

While our sign convention would suggest a downward moving drop would have negative w_c, w_T is positive because we treat it as a magnitude and apply signs as needed. As has long been recognized, the terminal velocity of a hydrometeor increases with size (although exactly how depends on the drag regime). In the context of (9), it is clear what c_1 is. It is the inverse of the depth over which gravity must act unopposed to yield the hydrometeor terminal kinetic energy.

Let us first make progress on (8) by examining a solution for the updraft case when $w_r(0)<0$ where the hydrometeor begins at rest and updrafts are weak. The solution to (8) is

$$w_c(t) = w_a - w_T \tanh\left(\frac{gt}{w_T} + \tanh^{-1}\left(\frac{w_a}{w_T}\right)\right) \tag{10}$$

Equation (10) is a known solution for describing the fall speed of a particle subject to a nonlinear drag force. Both (9) and (10) match the results from Stout *et al.* (1995) with the effects of buoyancy removed for example. This solution shows hydrometeors smoothly approach w_a with time and that they do so slower for larger w_T as expected.

Equation (10) does not hold for all updraft speeds, however, because the domain of the inverse hyperbolic tangent function, $\tanh^{-1}(x)$, is limited to $|x| < 1$. Thus, a second solution is required for strong updrafts, where the air velocity exceeds the magnitude of the terminal velocity of that droplet. Including the solutions for downdrafts, which are complicated slightly by the changing direction of the drag force, the relevant system of solutions are

$$w_c(t) = \begin{cases} w_a - w_T \tanh\left(\frac{gt}{w_T} + \tanh^{-1}\left(\frac{w_a}{w_T}\right)\right), & \text{if } 0 < w_a < w_T \\ w_a - w_T \coth\left(\frac{gt}{w_T} + \coth^{-1}\left(\frac{w_a}{w_T}\right)\right), & \text{if } w_a > w_T \\ +w_a - w_T \tan\left(\frac{gt}{w_T} + \tan^{-1}\left(\frac{w_a}{w_T}\right)\right), & \text{if } w_a < 0, t < \tau_{ff} \\ w_a - w_T \tanh\left(\frac{g(t-\tau_{ff})}{w_T}\right), & \text{if } w_a < 0, t > \tau_{ff} \end{cases}$$

$$\tau_{ff} = -\frac{w_T}{g}\tan^{-1}\left(\frac{w_a}{w_T}\right) \tag{11}$$

Equation (11a) is the same as (10) and is included for completeness. Equation (11b) approaches a steady state much faster than (10) for equivalent magnitudes of w_r (but for the appropriate sign) because F_f is comparatively large in a strong updraft. The downdraft solution (11c-d) is a piecewise function, with the solution form changing at a critical "free fall" time, $t = \tau_{ff}$ (11e), when the direction of F_f changes from downward to upward. At this moment, the droplet is moving downward at the same speed as the air, so it briefly enters a state of free fall before the solution proceeds in the same way as the weak updraft solution (11a) after that.

| Coupled Vertical Case

The uncoupled vertical case in the previous section is now compared to the case here in which the air is allowed to respond to the existence of hydrometeors (Fig. 1c). Coupling requires solving two equations of motion simultaneously. These are

$$\frac{dw_c}{dt} = -c_1 w_r \|w_r\| - g \tag{12}$$

$$\frac{dw_a}{dt} = \frac{1}{2} n C_T \pi r^2 w_r \|w_r\| \tag{13}$$

where n is the number density of droplets. Because the RHSs of (12-13) only include w_r, the solutions can be achieved by first recasting for an equation of motion for w_r by subtracting (13) from (12):

$$\frac{dw_r}{dt} = -(c_1 + \frac{1}{2} n C_T \pi r^2) w_r \|w_r\| - g \tag{14}$$

which is identical to the uncoupled case in (8) except for some constants. Following the same procedure as above, we arrive at a new terminal velocity

$$w_T(n, r, \rho_a) = \sqrt{\frac{g}{c_1 + \frac{1}{2} n C_T \pi r^2}} = \sqrt{\frac{8 \rho_w r g}{3(\rho_a + \rho_c) C_T}} = \sqrt{\frac{g}{c_2}} \tag{15}$$

The denominator, which inherits the extra constants in (14) can be rearranged using $\rho_c = \frac{4}{3} n \rho_w \pi r^3$, such that the total hydrometeor mass of the coupled system is recovered. We also see that a new "c-constant" has been defined, $c_2 = \frac{3(\rho_a + \rho_c) C_T}{8 \rho_w r}$. Equation (15) can be compared with (9). The presence of the condensate density in the terminal velocity means that it no longer solely depends on the droplet radius but also on the total mass (or total number) of drops in a volume of air. The factor by which w_T is reduced from the uncoupled to the coupled case can be understood by a factor we call γ. It is simply the ratio of (9) to (15)

$$\gamma = \sqrt{\frac{\rho_a}{\rho_a + \rho_c}} \tag{16}$$

Because of the implicit nature of w_T outside the Newtonian regime, γ is actually a lower bound on the reduction.

Figure 3 shows that increasing the amount of condensate in the atmosphere reduces the terminal velocity of the hydrometeors, but since $\rho_a >> \rho_c$ in most atmospheric conditions, this effect is small. However, in the case of even just a single 5 cm hailstone (which sets the upper limit on ρ_c in Fig. 3) at high altitudes where air density is low, this modification could be more than 80%. The same hailstone's calculated terminal velocity near the surface where air density is higher would be reduced by ~30%. The reduction in hydrometeor terminal kinetic energy for the new "c-constant" is the gain in kinetic energy of the air because the work done by gravity now acts on the center of mass of the laden system. Recall from Figure 1c that the net force on the laden system is just that from gravity because the frictional force is internal to the system. The more hydrometeors exist in the system, the more efficiently the gravitational potential energy loss of the drops is converted to kinetic energy of the air through friction. Another way to state this is that because in the long-time limit the air accelerates downward in the direction of motion of the falling hydrometeor(s), the relative velocity is reduced compared to the uncoupled case. As such, the frictional drag is reduced, and a slower terminal velocity is required to balance the drag. But, because the air has accelerated downward more, the net fall speed of hydrometeors relative to the ground may be higher than in the uncoupled case at long times.

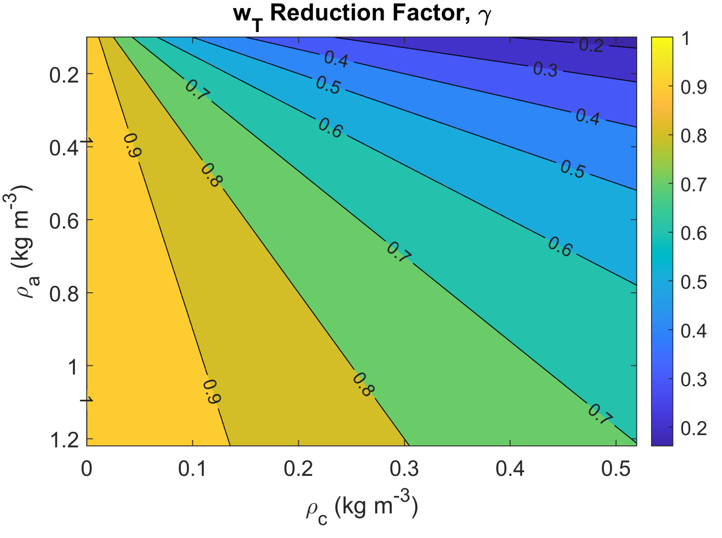

FIGURE 3 *The terminal velocity reduction factor for the Newtonian regime, γ, for various densities of air and drops.*

Solutions to (14) obtained similarly to (10) can be substituted back into (12-13) to become

$$\frac{dw_c}{dt} = c_1 w_T^2 \tanh^2\left(\frac{gt}{w_T} + \tanh^{-1}\left(\frac{w_a(0)}{w_T}\right) - g\right) \tag{17}$$

$$\frac{dw_a}{dt} = -\frac{1}{2} n C_T \pi r^2 w_T^2 \tanh^2\left(\frac{gt}{w_T} + \tanh^{-1}\left(\frac{w_a(0)}{w_T}\right)\right). \tag{18}$$

which have solutions, for initial conditions $w_c(0) = 0$ and arbitrary $w_a(0)$ for $w_a(0) < w_T$,

$$w_c(t) = -\gamma^2 w_T \left[\tanh\left(\frac{gt}{w_T} + \tanh^{-1}\left(\frac{w_a(0)}{w_T}\right)\right) - \frac{w_a(0)}{w_T}\right] - \frac{\rho_c}{\rho_a + \rho_c} gt \tag{19}$$

$$w_a(t) = w_a(0) + \frac{nC_T \pi r^2 w_T^3}{2g}\left[\tanh\left(\frac{gt}{w_T} + \tanh^{-1}\left(\frac{w_a(0)}{w_T}\right)\right) - \frac{w_a(0)}{w_T} - \frac{gt}{w_T}\right] \tag{20}$$

where we have only presented the equivalent of the first case in (11) but where it should be understood that similar case distinctions should be made here as there. These equations are certainly more complicated than the equations from the uncoupled vertical case, but there are some things in common between the two solutions. The most notable similarity is that in both solutions, equations (19) and (10), the argument of the hyperbolic tangent depends on the same coefficients, although those coefficients do have slightly different values. Thus, the acceleration proceeds in a similar manner to the uncoupled case, although modified by a more complicated prefactor.

In these solutions, the *tanh* functions describe the initial acceleration of the air and hydrometeors, but at long times, the linear-in-time terms dominate. The linear terms arise due to the loading of the air by the falling hydrometeors, and they are equivalent to the fully derived traditional loading force acting in the vertical (Bannon, 2002), given a subscript *l*,

$$F_l = -\frac{\rho_c}{\rho_a + \rho_c} g \tag{21}$$

Loading is negative, so ignoring effects from other forces, loading results in a gradual downward acceleration of the air. Because $w_r = w_c - w_a$ is constant at long times, air (and hydrometeors) eventually accelerate at F_l. Using (21) to rewrite (19-20) for emphasis,

$$w_c(t) = -\gamma^2 w_T \left[\tanh\left(\frac{gt}{w_T} + \tanh^{-1}\left(\frac{w_a(0)}{w_T}\right)\right) - \frac{w_a(0)}{w_T}\right] + F_l t \tag{22}$$

$$w_a(t) = w_a(0) - \frac{F_l}{g}\left[\tanh\left(\frac{gt}{w_T} + \tanh^{-1}\left(\frac{w_a(0)}{w_T}\right)\right) - \frac{w_a(0)}{w_T}\right] + F_l t \tag{23}$$

When this is done, we are left with an atypical interpretation of the physical system of air loaded with hydrometeors. The speed of the air has two components proportional to F_l, the latter being the traditional 'loading' and the former being what we will call for lack of a better term the 'lofting' which is directed upward (i.e. negative F_l) and arises due to transient acceleration of the system due to explicit hydrometeor momentum. The lofting term is always smaller than the loading term and so their sum never results in upward motion of the air.

Figure 4 shows traces of the dynamic evolution of the system for seven values of $w_a(t{=}0)$. These results use r=5 mm (such that $w_T \approx 15$ m s^{-1}) and a total ρ_c=10 g m^{-3}. First, we will consider the $w_a(0) \approx w_T$ case (light blue lines). Here hydrometeors very nearly maintain w_r=w_T at all times which means neither the acceleration of air nor the drops changes much in time. For the rapidly rising w_a(0)=20 m s^{-1} case, the hydrometeors are initially accelerated upward and the air strongly accelerated downward. For the slowly rising cases, hydrometeors slowly approach their terminal relative speed and the air monotonically approaches a constant acceleration due to loading. The downdraft cases show nonmonotonic behavior and the longest approaches to equilibrium behavior. As they are allowed to accelerate, the hydrometeors approach a point at which they are in free fall (Fig. 4a) and the air is simultaneously completely unloaded (no air acceleration; Fig. 4b) before following the same qualitative evolution as the updraft cases thereafter.

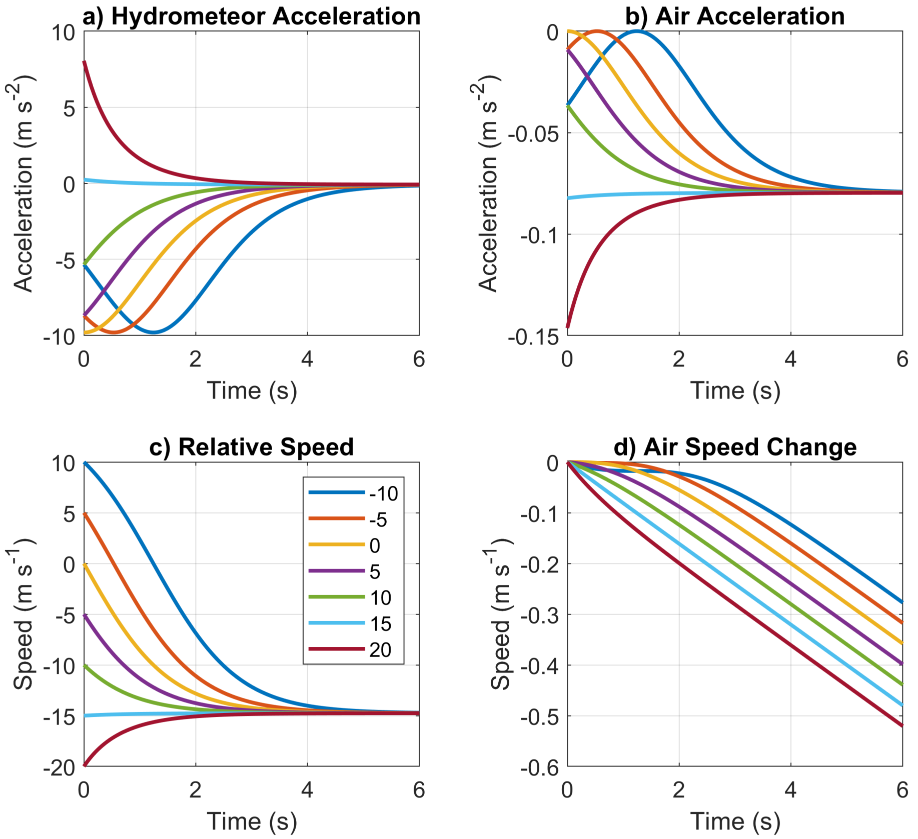

FIGURE 4 *Acceleration and vertical speed traces for the vertical coupled case for different initial relative speeds (shown in the legend with units of m s $^{-1}$). Accelerations of the hydrometeors and air are shown in the top row. The relative speed evolution of the hydrometeors as a function of initial air speed is shown in c) and the air speed change is shown in d).*

The hydrometeors approach terminal velocity in about the same amount of time as in the uncoupled vertical case (several seconds; Fig. 4c), but now there is a continuous constant acceleration that is a result of hydrometeor loading. This loading also results in a downward acceleration of the air, and at long times, the air and hydrometeor accelerations are identical, and equal to the value in (21).

| Uncoupled 2-Dimensional Case

The previous physical cases were incomplete because the frictional force, (3), is a vector quantity and they only considered motion in one direction. Here, we consider 2-dimensional motion (like Fig. 1d). In many physical systems, a force vector would decompose, and components could be treated separately, but (3) includes a magnitude term which precludes separation. The momentum equations are

$$\frac{du_c}{dt} = -c_1 u_r \|v_r\| \tag{24}$$

$$\frac{dw_c}{dt} = -c_1 w_r \|v_r\| - g \tag{25}$$

Because of the magnitude term, the acceleration in each direction is directly coupled to the relative motion in the other direction. No explicit solutions have been found to (24-25). First, we examine a grossly approximate solution that points out one important feature. In many cases in the atmosphere, the magnitude of the relative velocity is approximately the terminal velocity. Making this approximation and using (9) for simplicity means that (24-25) becomes

$$\frac{du_c}{dt} = -c_1 u_r w_T \tag{26}$$

$$\frac{dw_c}{dt} = -c_1 w_r w_T - g \tag{27}$$

The solutions of (26-27) are

$$u_c(t) = u_a(1 - e^{-\sqrt{c_1 g}t}) \tag{28}$$

$$w_c(t) = (w_a + w_T)(1 - e^{-\sqrt{c_1 g}t}) \tag{29}$$

These solutions are not particularly interesting except in one important regard – the timescales of the adjustment of the horizontal wind involve gravity despite gravity's only acting on the vertical momentum equation [i.e. (27)]. The result is that hydrometeors rapidly equilibrate to the speed of the *horizontal* wind due to the relative largeness of gravity acting in the *vertical*. In addition to the uncoupled horizontal solutions, Fig. 2 also shows cases of (28) which illustrate the many orders of magnitude faster adjustment times for horizontal motion when settling. So, while incomplete, conceptual and numerical models that assume hydrometeors act as horizontal passive tracers of the air do not behave nearly as poorly as the uncoupled horizontal case would suggest. However, we will point out that the 1 cm sphere still takes 10 s to reach 99% of the horizontal wind speed (of 1 m s^{-1}) and ~27 s to reach the horizontal speed to within double machine precision.

We return to (24-25). We can understand the qualitative nature of its solutions through a simple phase plain analysis. It is straightforward to show that there exists a stable equilibrium point, (u_c^*, w_c^*), whose coordinates are

$$(u_c^*, w_c^*) = (u_a, w_a - w_T) \tag{30}$$

as we would expect them to be. Solving equation (24-25) numerically for a range of initial conditions with u_a=0 m s^{-1}, w_a=3 m s^{-1}, and w_T=10 m s^{-1} demonstrates that trajectories converge to this equilibrium point (Fig. 5). We also observe that for certain initial conditions (e.g. the blue line in Fig. 5) where $u_a(t{=}0)$ is large and $w_a(t{=}0)$-w_T is small, the vertical velocity magnitude of the condensate *decreases* initially, but after passing through the curve where $g > \|\mathbf{F_f} \cdot \mathbf{k}\|$, it begins to increase until converging to the equilibrium point.

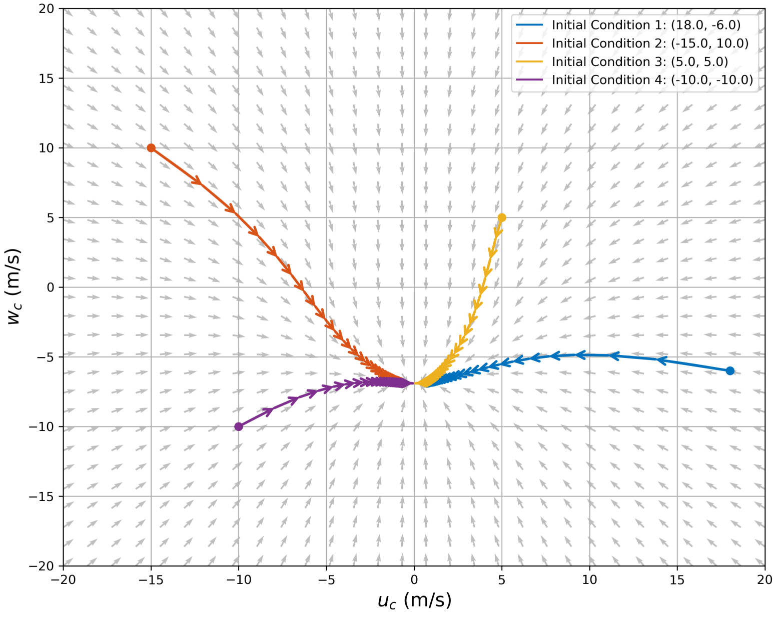

FIGURE 5 Tendencies of condensate velocity components (vectors of unit length). Trajectories of velocity components for four characteristic initial conditions (colors). Initial conditions are given as (u_c, w_c)

The coupled nature of (24-25) implies that terminal settling speeds of hydrometeors must be slowed in the presence of a hydrometeor-relative horizontal wind. For example, when hydrometeors settle through a layer of constant vertical shear of the horizontal wind, the drop will always feel a relative horizontal speed. The factor by which the terminal speed is reduced relative to when u_r=0 m s^{-1} can be found by setting the LHS of (25) to zero and solving for w_r. It is

$$\beta = \sqrt{\frac{\sqrt{\alpha^4 + 4} - \alpha^2}{2}} \tag{31}$$

where $\alpha = \frac{u_r}{w_T(u_r=0)}$, the horizontal relative velocity normalized by the uncoupled terminal speed [i.e. (9)]. The β factor is always less than one and decreases with α (Fig 6a). As such, fall velocities are slowed more for small drops and strong horizontal winds. However, the rapid equilibration of small drops (see Fig. 2), results in β~1 on most timescales for those drops, since u_r rapidly goes to 0. Equation (31) presents a reasonably general result; for a thorough discussion of the case of a hydrometeor falling through a layer of constant shear, see Khain and Pinsky (1995) or Ingel' (2012). Finally, we will note that by assumption, all drops are spheres. In reality, the 2-dimensional case is complicated by the deformation of drops (Allende and Bec, 2023). Spheroids would have different measured radii in different directions and therefor different 'c-constants' in (24-25).

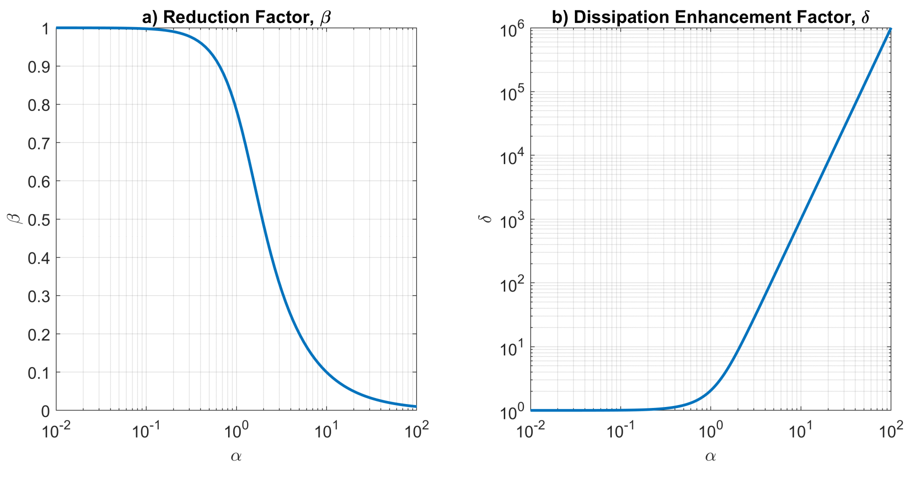

FIGURE 6 *a) The β factor by which w_T is reduced in the presence of a horizontal wind as a function of the α parameter (the ratio of relative horizontal velocity to the terminal fall speed). b) The δ factor by which D is enhanced in the presence of a horizontal wind.*

| Coupled 2-Dimensional Case

The final case is that of the fully coupled system. By noticing the relationship between c_1 and c_2, and pulling in (16) to recast the factors expected from for the acceleration of the air like (13), the relevant equations of motion are

$$\frac{du_c}{dt} = -c_1 u_r \|v_r\| \tag{32}$$

$$\frac{dw_c}{dt} = -c_1 w_r \|v_r\| - g \tag{33}$$

$$\frac{du_a}{dt} = c_2(1-\gamma^2)u_r\|v_r\| \tag{34}$$

$$\frac{dw_a}{dt} = c_2(1-\gamma^2)w_r\|v_r\| \tag{35}$$

Here, again, we are unable to solve this system generally. However, it should be clear from the previous section that interesting coupling will occur. The units of the RHSs of (32) are all inverse length times a velocity squared which reduces to an acceleration (as it must). The meaning in (32-33) is clear as c_1 is the depth over which gravity acts unopposed on hydrometeors to achieve a terminal kinetic energy and serves to scale the acceleration from friction. However, the meaning of the $c_2(1-\gamma^2)$ in (34-35) is less obvious. It still has units of inverse length and determines the intensity of the acceleration from friction. In the trivial case with no hydrometeors, ρ_c=0 andγ=1, the air does not accelerate because the effective depth is infinite. When ρ_c>0, γ<1, the effective depth is finite meaning continued settling will accelerate the air. Conceptually then, $c_2(1-\gamma^2)$ may be thought of as the depth air settles in the time it takes the drops to achieve their terminal kinetic energy.

As an example of the potential impact of coupling, we invoke a contrived case with $r = 1\mu m$ and a concentration of 1000 cc^{-1}. We force a background wind, $\mathbf{v_a}$, the magnitude of which equals w_T at 1.17 m s^{-1} with period 2 s that oscillates coherently and sinusoidally in both directions. We calculate the forcing needed to maintain these winds and add them to the RHS of (34-35), then integrate all four momentum equations forward in time for five periods. Purely forced results are shown in yellow in Fig. 7, and simulated results are shown in blue and red. Figure 7 shows that the hydrometeors serve as a damper on the wind speed oscillations in both the vertical and horizontal. Not only is the magnitude of the resulting horizontal wind speed oscillations lessened by the hydrometeors, but the phasing is altered as the peak speed occurs earlier than the forcing would dictate alone. For their part, the hydrometeors oscillate horizontally with a much lesser magnitude than the wind and do so at a phase delay of about 1/4 the wave period (which is unique to the setup used and not a general result). In the vertical, the relative fall speed peaks earlier in the 2D coupled case than does the 1D coupled case in which we only consider w_r when calculating $\boldsymbol{F_f}$ (as a way to contrast the effect of full 2D coupling with that in the previous section). The hydrometeor fall speeds are reduced relative to the unperturbed case slightly more in the 2-dimensional coupling case than in the 1-dimensional coupling.

To close this section, we will point out that the system of equations we solve above lacks a horizontal pressure gradient term which will likely be important in reality in the case of strong horizontal accelerations. Its exclusion is in keeping with our assumption of perfect hydrostatic balance in the vertical implying no anomalous pressure gradient but is a strongly simplifying assumption rather than physical. Full numerical models will likely be needed to understand the countervailing effects of anomalous pressure fields.

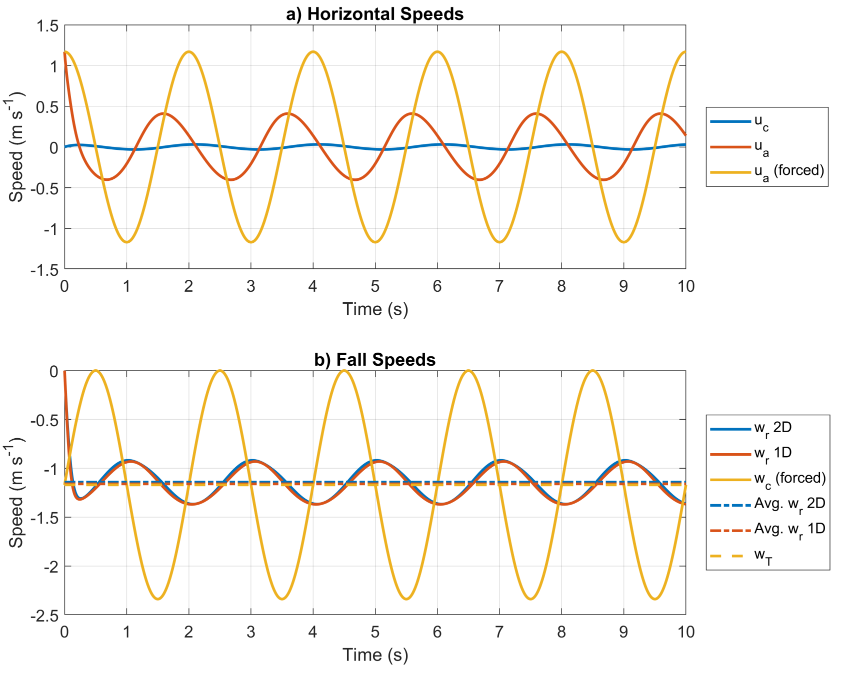

FIGURE 7 *Speeds in the circular turbulence experiment. Yellow lines show the result of the system responding only to the circular forcing only. Panel a) shows horizontal speeds. The red and blue lines show full-physics results. Panel b) shows vertical relative speeds of hydrometeors in blue. The red line shows the result if air and hydrometeors are only coupled in the vertical. Dashed lines show average or calculated fall speeds.*

| Dissipation

As a final calculation, we will use what we have learned above to address an incompleteness in Igel and Igel (2018) who discussed the energetic nature of frictional heating by hydrometeors falling at w_T. They were unable to calculate the frictional dissipation rate as a drop accelerated toward w_T and only presented steady state results. The dissipation rate per unit mass, D, in quiescent air is

$$D = \frac{d}{dt} KE_c + \frac{d}{dt} PE_c \tag{36}$$

where KE is the kinetic energy and PE is the potential energy. Beginning from the vertical uncoupled case for simplicity, (36) becomes

$$D = w_c \frac{dw_c}{dt} + g w_c \tag{37}$$

Then, substituting in (8) and noting changes in kinetic energy of the air do not contribute to dissipation, (37) becomes

$$D = w_c(-c_1 w_c^2 - g) + g w_c = -c_1 w_c^3 \tag{38}$$

As a check, we note that when $-w_c = w_T$, then $D = g w_T$ which matches the result in Igel and Igel (2018). The solutions for $w_c(t)$ from (11) may be substituted into (38) to examine the approach to steady state dissipation.

The full D may be calculated by forming a vector in the uncoupled 2-dimensional case, (24), and inserting into (36). It is

$$D = c_1 \|\mathbf{v_c}\|^3 \tag{39}$$

By extension, if we relax the assumption that $w_a = 0$, then $\mathbf{v_c}$ in becomes $\mathbf{v_r}$ in (39).

Previous dissipation calculations have made the assumption that all drops fall at their terminal speed (Pauluis *et al.*, 2000; Pauluis and Dias, 2012; Romps, 2008). How large an error is this for drops falling and subjected to a vertically sheared or horizontally accelerating horizontal wind or turbulent fluctuations? We may use the definition of α and β to rewrite (39) as

$$D = c_1 [\sqrt{(\alpha w_T (u_r = 0)^2 + \beta w_T (u_r = 0)^2}]^3 \tag{40}$$

or as

$$D = c_1 (\alpha^2 + \beta^2)^{3/2} w_T (u_r = 0)^3 = c_1 \delta w_T (u_r = 0)^3 \tag{41}$$

where we have defined $\delta = (\alpha^2 + \beta^2)^{3/2}$ as the dissipation enhancement due to horizontal relative motion of drops. Because we cannot characterize u_r generally, we cannot know how large an error is introduced by assuming dissipation occurs only due to settling. But, it is clear from Fig. 6b that *proportionally* this error might be very large especially in cases of slow terminal settling speeds when α might conceivably be large.

Discussion and Conclusions

Here, we have systematically dealt with momentum equations of hydrometeors affected by friction with air. In considering a wide range of physically limited cases, we discussed several important physical results. These are:

- In the absence of gravity, equilibration times of weakly horizontally moving air and large hydrometeors can be ~1000 s. However, when hydrometeors are allowed to fall in a gravitational field, their horizontal equilibration times are approximately equivalent to their equilibration times in the vertical (see Fig. 2).

- When the coupled air-hydrometeor system is considered, the terminal velocity of hydrometeors depends on the total mixing ratio of drops, not just their size (see (15)).
- Hydrometeors act as a damper on turbulent air. The vector nature of friction means that turbulent air which induces horizontal friction in the system can meaningfully reduce the air or ground relative fall velocity of hydrometeors (e.g. Fig. 7).
- Frictional dissipation of hydrometeor total energy depends on the third power of the particle velocity (see (38)).

While we have largely considered physical implications, some of our motivation was eventual model improvement. We would suggest that explicit hydrometeor momentum is likely to be most impactful for models with very short timesteps and fine grids (like DNS) or detailed treatment of hydrometeor interactions (like super droplet methods), for simulations of deep convection where hydrometeor mass mixing ratios are particularly large, and especially for simulations in which hail is a significant contributor to internal air dynamics or surface accumulation of precipitation.

Appendices

| Appendix A

The drag coefficient, (4), depends on the velocity of the droplet in complicated ways, which makes solving (7) with a variable drag coefficient very difficult. Thus, the same technique laid out in Stout *et al.* (1995) for the uncoupled vertical case was used here in all but the uncoupled horizontal case, where the constant drag coefficient is chosen based on the terminal velocity of a droplet of that radius. The steps below indicate how that drag coefficient value was determined, by substituting the expression for the terminal velocity, (9), into the drag coefficient expression. The equation that gives this "terminal drag coefficient", (45), is a quartic polynomial with one positive root, and that root was found using a bisection algorithm. If a different expression for the drag coefficient was used, then the process laid out below would produce a different final result, but the same steps would be carried out.

The drag coefficient, (4), at terminal velocity is

$$C = \frac{12\mu}{\rho_a r w_T} + 4.4\sqrt{\frac{\mu}{2\rho_a r w_T}} + 0.44 \tag{42}$$

and can be rewritten by replacing w_T

$$C = \frac{12\mu}{r}\sqrt{\frac{3C}{8\rho_a \rho_w r g}} + 4.4\sqrt{\frac{\mu}{2r}}\left(\frac{3C}{8\rho_a \rho_w r g}\right)^{1/4} + 0.44 \tag{43}$$

By gathering terms into a and b

$$C = a\sqrt{C} + bC^{1/4} + 0.44 \tag{44}$$

allow us to arrive at a solvable polynomial

$$0 = -\xi^4 + a\xi^2 + b\xi + 0.44 \tag{45}$$

where $\xi^4 = C$.

Figure 8 shows the numerically modeled percent error from the unapproximated drag coefficient with a time varying velocity introduced when assuming $C(v_r(t)) = C_T(w_T)$ for drops of different sizes and two different $v_a(0)$ and for $w_r(0) = 0$ m s^{-1}. For small drops, the error is initially a few tens of percent but transient. For large drops, the error is always extremely small but lasts a few seconds.

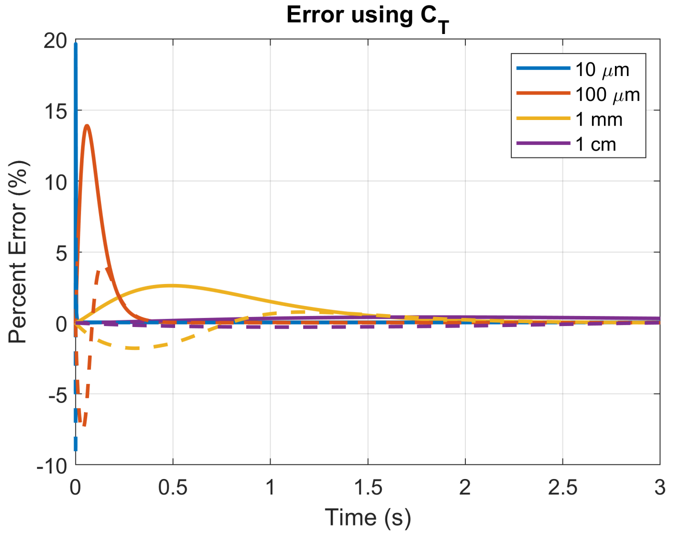

FIGURE 8 Percent error when using C=C_T at all times for w_a = 0 m s^{-1} (solid lines) and when w_a=w_T (dashed lines). w_T is calculated with (9).

references

Allende, S. and Bec, J. (2023). Velocity and acceleration statistics of heavy spheroidal particles in turbulence. *Journal of Fluid Mechanics*, 967. doi:10.1017/jfm.2023.508.
URL `http://dx.doi.org/10.1017/jfm.2023.508`

Amanbaev, T. R. (2024). Rain Drop Motion in an Atmosphere Containing Aerosols Particles. *Izvestiya, Atmospheric and Oceanic Physics*, 60 (1). doi:10.1134/s0001433824700014.
URL `http://dx.doi.org/10.1134/S0001433824700014`

Bannon, P. R. (2002). Theoretical Foundations for Models of Moist Convection. *Journal of the Atmospheric Sciences*, 59 (12). doi:10.1175/1520-0469(2002)059<1967:tffmom>2.0.co;2.
URL `http://dx.doi.org/10.1175/1520-0469(2002)059<1967:TFFMOM>2.0.CO;2`

Chen, S., Yau, M. K. and Bartello, P. (2018). Turbulence Effects of Collision Efficiency and Broadening of Droplet Size Distribution in Cumulus Clouds. *Journal of the Atmospheric Sciences*, 75 (1). doi:10.1175/jas-d-17-0123.1.
URL http://dx.doi.org/10.1175/JAS-D-17-0123.1

Garrett, T. J., Singh, D. K. and Pardyjak, E. R. (2025). Settling and Rotation of Frozen Hydrometeors in Turbulent Air. *Geophysical Research Letters*, 52 (12). doi:10.1029/2025gl114780.
URL http://dx.doi.org/10.1029/2025GL114780

Good, G., Ireland, P., Bewley, G., Bodenschatz, E., Collins, L. and Warhaft, Z. (2014). Settling regimes of inertial particles in isotropic turbulence. *Journal of Fluid Mechanics*, 759. doi:10.1017/jfm.2014.602.
URL http://dx.doi.org/10.1017/jfm.2014.602

Igel, M. R. and Igel, A. L. (2018). The Energetics and Magnitude of Hydrometeor Friction in Clouds. *Journal of the Atmospheric Sciences*, 75 (4). doi:10.1175/jas-d-17-0285.1.
URL http://dx.doi.org/10.1175/JAS-D-17-0285.1

Ingel', L. K. (2012). Nonlinear interaction between two components of motion upon precipitation of a heavy particle in a shear flow. *Technical Physics*, 57 (11). doi:10.1134/s1063784212110126.
URL http://dx.doi.org/10.1134/S1063784212110126

Khain, A. P. and Pinsky, M. B. (1995). Drop Inertia and Its Contribution to Turbulent Coalescence in Convective Clouds. Part I: Drop Fall in the Flow with Random Horizontal Velocity. *Journal of the Atmospheric Sciences*, 52 (2). doi:10.1175/1520-0469(1995)052<0196:diaict>2.0.co;2.
URL http://dx.doi.org/10.1175/1520-0469(1995)052<0196:DIAICT>2.0.CO;2

Loftus, K. and Wordsworth, R. D. (2021). The Physics of Falling Raindrops in Diverse Planetary Atmospheres. *Journal of Geophysical Research: Planets*, 126 (4). doi:10.1029/2020je006653.
URL http://dx.doi.org/10.1029/2020JE006653

Makarieva, A. M., Gorshkov, V. G., Nefiodov, A. V., Sheil, D., Nobre, A. D., Bunyard, P., Nobre, P. and Li, B. (2017). The equations of motion for moist atmospheric air. *Journal of Geophysical Research: Atmospheres*, 122 (14). doi:10.1002/2017jd026773.
URL http://dx.doi.org/10.1002/2017JD026773

Maxey, M. R. (1987). The gravitational settling of aerosol particles in homogeneous turbulence and random flow fields. *Journal of Fluid Mechanics*, 174. doi:10.1017/s0022112087000193.
URL http://dx.doi.org/10.1017/S0022112087000193

Montero-Martínez, G., Kostinski, A. B., Shaw, R. A. and García-García, F. (2009). Do all raindrops fall at terminal speed? *Geophysical Research Letters*, 36 (11). doi:10.1029/2008gl037111.
URL http://dx.doi.org/10.1029/2008GL037111

Ooyama, K. V. (2001). A Dynamic and Thermodynamic Foundation for Modeling the Moist Atmosphere with Parameterized Microphysics. *Journal of the Atmospheric Sciences*, 58 (15). doi:10.1175/1520-0469(2001)058<2073:adatff>2.0.co;2.
URL http://dx.doi.org/10.1175/1520-0469(2001)058<2073:ADATFF>2.0.CO;2

Pauluis, O., Balaji, V. and Held, I. M. (2000). Frictional Dissipation in a Precipitating Atmosphere. *Journal of the Atmospheric Sciences*, 57 (7). doi:10.1175/1520-0469(2000)057<0989:fdiapa>2.0.co;2.
URL http://dx.doi.org/10.1175/1520-0469(2000)057<0989:FDIAPA>2.0.CO;2

Pauluis, O. and Dias, J. (2012). Satellite Estimates of Precipitation-Induced Dissipation in the Atmosphere. *Science*, 335 (6071). doi:10.1126/science.1215869.
URL http://dx.doi.org/10.1126/science.1215869

Pielke Sr., R. A. (1984). *Mesoscale Meteorological Modeling*. : Elsevier.

Pruppacher, H. and Klett, J. D. (1997). *Microphysics of Clouds and Precipitation: With an Introduction to Cloud Chemistry and Cloud Electricity*. : .

Romps, D. M. (2008). The Dry-Entropy Budget of a Moist Atmosphere. *Journal of the Atmospheric Sciences*, 65 (12). doi:10.1175/2008jas2679.1.
URL `http://dx.doi.org/10.1175/2008JAS2679.1`

Shapiro, A. (2005). Drag-Induced Transfer of Horizontal Momentum between Air and Raindrops. *Journal of the Atmospheric Sciences*, 62 (7). doi:10.1175/jas3460.1.
URL `http://dx.doi.org/10.1175/JAS3460.1`

Spengler, T., Egger, J. and Garner, S. T. (2011). Retrieveal of Thermal and Microphysical Variables in Observed Convective Storms. Part 1: Model Development and Preliminary Teting. *Journal of the Atmospheric Sciences*, 42. doi:10.1175/2010JAS3582.1.

Stout, J. E., Arya, S. P. and Genikhovich, E. L. (1995). The Effect of Nonlinear Drag on the Motion and Settling Velocity of Heavy Particles. *Journal of the Atmospheric Sciences*, 52 (22). doi:10.1175/1520-0469(1995)052<3836:teondo>2.0.co;2.
URL `http://dx.doi.org/10.1175/1520-0469(1995)052<3836:TEONDO>2.0.CO;2`

data availability

No data created.

acknowledgements

The authors acknowledge support from NSF ASG 2025103. They also thank two anonymous reviewers for their diligent attention to detail.

conflict of interest

The authors claim no conflicts.

GRAPHICAL ABSTRACT

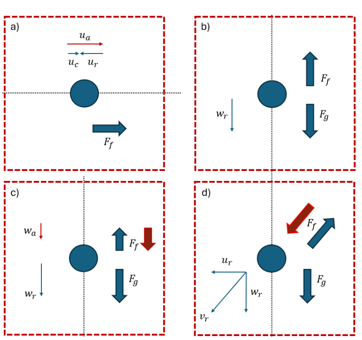

Momentum equations of hydrometeors and air are explored in several limiting cases. In each case, we focus on case-specific modifications of terminal fall speeds.